ICONHIC2022
3rd International Conference on Natural Hazards & Infrastructure
5-7 July 2022, Athens, Greece

Geotechnical Assessment of the Pore Water Pressure Build-up in Izmir During the October 30, 2020, Samos Earthquake

Anna Chiaradonna, Ph.D.[1], Paola Monaco
University of L'Aquila, Italy

Eyyub Karakan, Ph.D.
Kilis 7 Aralik University, Turkey

Giuseppe Lanzo, Ph.D.
Sapienza University of Rome, Italy

Alper Sezer, Ph.D.
Ege University, Izmir, Turkey

Mourad Karray, Ph.D.
Universitè de Sherbrooke, Quebec, Canada

ABSTRACT

On October 30, 2020, a damaging earthquake of moment magnitude 6.6 struck about 14 km northeast of the island of Samos, Greece, and about 70 km from the center of the city of Izmir in Turkey. Even though the epicenter was relatively far away, the effects of the seismic event in the highly populated city center of Izmir were destructive causing over 100 fatalities and significant structural damage. Apart from the site effects that characterized this earthquake, a few liquefaction manifestations were observed during the event. This paper documented the pore water pressure build-up observed in the Bayrakli district after the October 30, 2020 earthquake. Approximate properties of the foundation soils were defined based on a fragmentary reconstruction of the field investigation before the construction of the building. The safety factor against liquefaction was then estimated and it was consistent with the absence of liquefaction manifestation in the area. Simplified prediction of the expected excess pore water pressure based on a simple relationship as a function of safety factor allowed preliminary assessment of the mechanism that is behind the observed phenomena. The proposed methodology is particularly convenient for rapid screening of the expected earthquake-induced effects since it can be directly applied to the safety factor without the identification of additional input data.

Keywords: 2020 Samos earthquake, site effects, liquefaction, pore water pressure

INTRODUCTION

Earthquake-induced soil liquefaction is among the major threats that affect high populated urban communities and infrastructures. Several cases were reported in the past, e.g., Marina District (San Francisco) after the 1989 Loma Prieta earthquake (e.g., Boulanger et al., 1997; Kayen et al., 1998) and Kobe city after the 1995 Kobe earthquake (Cubrinovski et al., 1996; 2000). Another significant example is the city of Christchurch, which was the core of massive liquefaction phenomena after the 2010-2011 Canterbury earthquake sequence (Cubrinovski et al., 2018). More recently, the M=7.5 September 28, 2018, Sulawesi earthquake affected the

[1] Department of Civil, Construction-Architectural and Environmental Engineering, anna.chiaradonna1@univaq.it

coastal city of Palu, grown around the Palu river, where at least 2000 people lost their lives (Sahadewa et al., 2019).

Izmir, which is the third-largest city of Turkey by the number of inhabitants (about 4 million) and the second biggest port after Istanbul, was also recently struck by a damaging earthquake of moment magnitude 6.6 on October 30, 2020. The epicenter of the seismic event was located about 14 km northeast of the island of Samos, Greece, and about 70 km from the center of Izmir (Figure 1a). Despite the remarkable distance from the epicenter, the seismic event caused 117 fatalities, over 1030 injuries, and significant structural damage (Cetin et al., 2020). Cetin et al. (2021), Karakan et al. (2021) and Chiaradonna et al. (2022) analyzed the distribution of the damage and highlighted the correlations with the local site conditions and double resonance effects. Assessment of the damage distribution also revealed that the Bornova, Karşıyaka, and Bayrakli districts located in the highly-populated city center suffered most of the damage (Figure 1b).

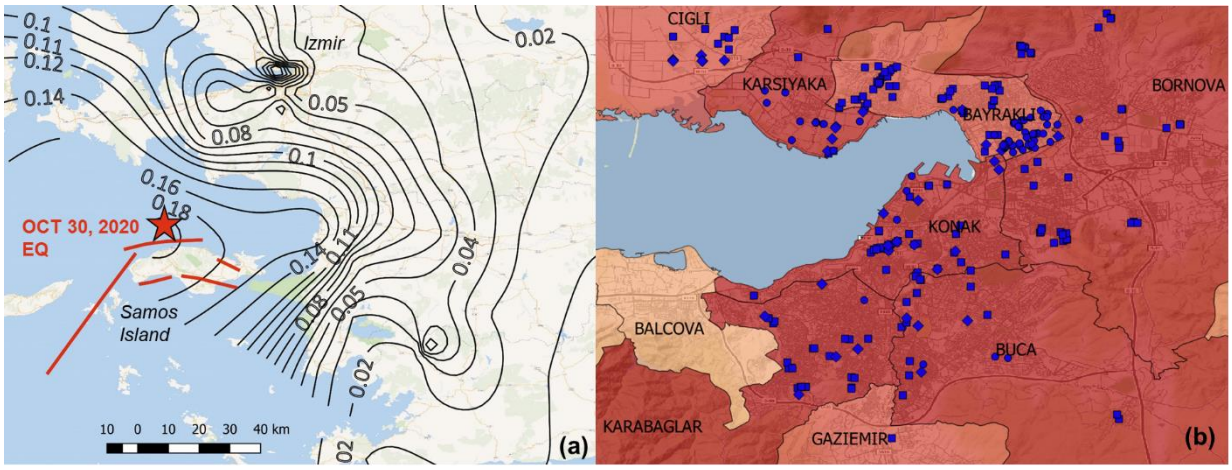

Figure 1. *The epicenter of the October 30, 2020 earthquake and contours of the recorded PGA (a) and districts in the city center of Izmir with damage observations (blue points) (b)*

Izmir is settled along the eastern coasts of the Aegean Sea, near the Gulf of Izmir. The city overlies alluvial deposits susceptible to liquefaction. Young alluvium (Holocene) and the fan delta with shallow marine deposits, confined and controlled by the Izmir fault to the south and the Karşıyaka-Bornova fault to the north, constitute the highest sediments in the basin. In the middle part of the basin, the fill exceeds 300 meters in thickness. Previous studies quantified the soil liquefaction susceptibility of the region and estimated values of post-liquefaction settlements (Sezer et al., 2008). Karakan & Altun (2016) performed cyclic triaxial tests on sand-silt mixtures from Bayrakli, underlying that an earthquake of 7.5 magnitude can lead mixtures of 40% silt content to liquefaction, after 20 cycles. Özyalin & Tunçel (2021) applied MASW method to evaluate average shear wave velocity in the top 30 m, and later carried out liquefaction analyses on 50 profiles from Izmir. It was stressed that the areas with high liquefaction potential cover the Bornova Plain and the coastal areas in the vicinity of Izmir Bay. Prepared maps show that areas with high liquefaction potential are in agreement with information derived from the distribution and stratification of alluvial units in the region.

This paper focuses on the manifestations of liquefaction and excess pore water pressure that occurred during the October 30, 2020 earthquake. A brief description of the seismic event and related liquefaction manifestations as reported in previous studies are summarized in the next section. A focus is then related to the Izmir city center where pore water pressure build-up was observed in the foundation soils. During the earthquake, water rose to basement level from stone columns below a residential building located in the Bayrakli district, the case was documented and quantitatively interpreted. Assessment of the safety factor against liquefaction and prediction of the expected excess pore water pressure using a simple relationship provides an insight into the understanding of the observed phenomenon.

THE OCTOBER 30, 2020 EVENT AND LIQUEFACTION MANIFESTATIONS

The October 30, 2020 earthquake occurred at 13:51 UTC on the northern coasts of Samos Island, at coordinates (37.9001°N, 26.8057°E) and a focal depth of 12 km according to the Institute of Geodynamics, National Observatory of Athens. The Peak Ground Acceleration (PGA) recorded on soft rock was approximately 0.173g at the closest station located in Samos Prefecture (Greece), 19 km from the epicenter (Kalogeras et al., 2020). Figure 1a shows the contours of the peak ground acceleration (largest of the two horizontal components) based on 160 records obtained from the Turkish seismic network (AFAD; www.afad.gov.tr).

Primary and secondary environmental effects triggered by the earthquake in Samos Island were documented by Mavroulis et al. (2021) based on field survey and InSAR analysis. Among the secondary effects, liquefaction phenomena were observed in the coastal area of Malagari, at the southern Vathy bay (Figure 2a). The manifestations consisted of ground cracks and ejection of a liquefied mixture of water and sand along cracks. Lateral spreading was observed, resulting in subsidence along the coast.

In the north of the Island, Cetin et al. (2020) reported damage to buildings likely affected by lateral spreading towards the seafront in the neighborhood of Vyrsodepsia in Karlovasi (Figure 2b). In this case, no evidence of liquefaction was observed nearby, but the cracks and local conditions (level/mildly sloping ground, shallow water table, free face to the sea) seem to point towards the hypothesis of lateral spreading. The same Authors reported presumably sand ejecta in Karlovasi and Malagari ports.

Along the Western coast of Turkey, several places were visited by several research groups but no surface manifestations were documented (Cetin et al., 2020). The only exception is represented by the sand boils observed along the shores of the Icmeler and Gulbahce districts (Figure 2c). The ejected sand is mainly clean and uniform sand (Cetin et al., 2020). Overall, the liquefaction manifestations associated with the 2020 seismic event are limited and characterized by minor entities.

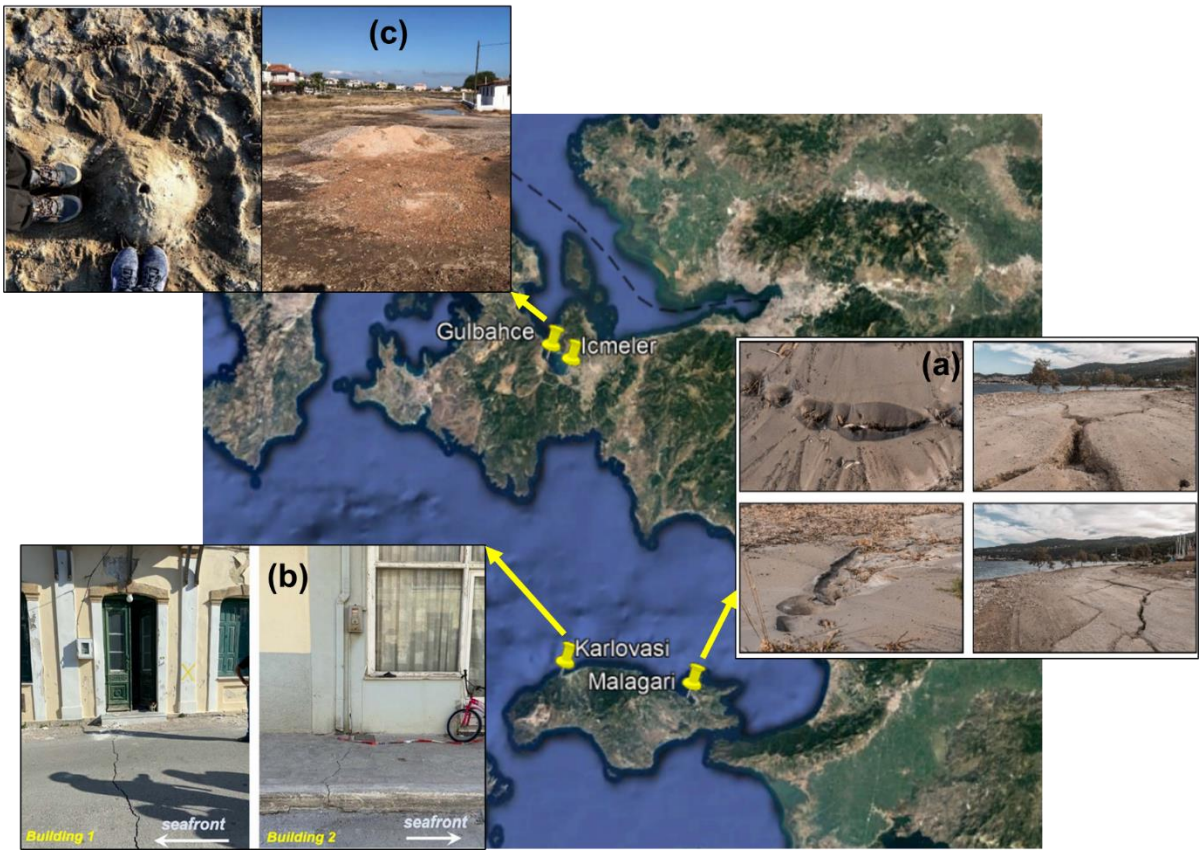

Figure 2. *Liquefaction manifestations detected after the October 30, 2020 earthquake (photos from* Cetin et al., 2020; Mavroulis et al., 2021)

No liquefaction evidence was reported in Izmir. The Department of the earthquake of the Ministry of Interior of the Turkish government installed a dense seismograph array (16 seismic stations in the bay and a total of 36 in Izmir Province) that successfully recorded strong ground motions during the events that occurred in the last decade. Figure 3a presents the distribution of the seismic stations in the Izmir region, classified upon subsoil class based on EC8. The maximum acceleration of the earthquake on the rock subsoil (class A) around the Izmir city center was generally less than 0.06 g. Conversely, the stations located on thick alluvial deposits in the center of the valley indicate accelerations that reach 0.15 g around station 3519 and 0.11 g near station 3521.

The low intensity of the recorded ground shaking can justify the absence of liquefaction evidence, even though the alluvial deposits of the plain are susceptible to liquefaction. Nevertheless, 10 groundwater wells were being monitored in the Bayraklı district, in the vicinity of the majority of the collapsed buildings (Figure 3b). Groundwater level, temperature, and electrical conductivity changes were monitored at 1h intervals in 5 wells by Uzelli et al. (2021). A trend of rising groundwater level to a height of 10 cm was observed. The water levels returned to their original height about 7 to 10 days after the earthquake. During the earthquake swarm (from October 30 to November 7, 2020), instantaneous level changes caused by aftershocks were also observed in some wells (Uzelli et al., 2021).

In the same Bayraklı district, a water eruption was observed in the basement of a building (Figure 3b – red arrow), which is documented in the next section.

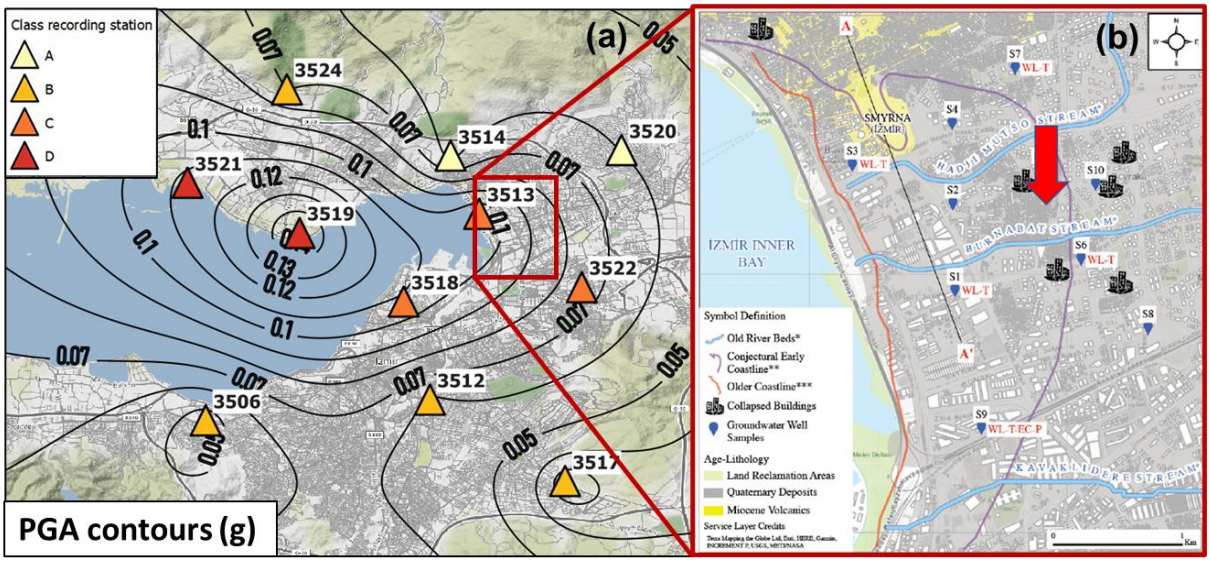

Figure 3. *Contours of the recorded PGA of the October 30, 2020 earthquake in Izmir Bay (a) and monitoring wells and collapsed buildings in the Bayrakli district (The red arrow identifies the building where water eruption was observed) (b) (modified after Uzelli et al., 2021)*

PORE PRESSURE BUILD-UP IN THE FOUNDATION SOILS IN BAYRAKLI

The considered building was a 9-story ~27-m reinforced concrete (RC) structure, which is 23 m wide (N-S) and 30 m long (E-W), located in the Bayraklı district (Figure 3b). This residential structure is 2.6 km far from the shoreline and east of the recording station 3513. The groundwater table is detected to be 1 m below the ground level. Data about the foundation and the foundation soils are limited and retrieved from the geological-geotechnical investigation report dated back to the building construction. The raft foundation covers a total area of 700 m^2 and the foundation depth is 3 m from the ground level. To prevent liquefaction, 199 vertical drains 9 m long and with a diameter of 30 cm were built under the foundation. The spacing among the columns varies between 1-2.5 m, while the size of gravel used for the columns ranges between 0.5-4 cm (Figure 4).

Figure 4. *Vertical drains installed in the foundation soils of the building during construction works (Sezer, 2020)*

After the 2020 Samos earthquake, water came out from the columns, and it was visible on the floor of the basement. The embedded story is a property without finishes, so the erupted water was visible, and eyewitnesses referred that the floor remained wet for several days after the event. Partial damage was also observed on the first floor of the structure so that carbon fiber reinforced columns were installed as remediation measurements. No sand boils, liquefaction manifestations or bulging were observed in the vicinity of the structure or the surrounding areas.

Soil stratigraphy

The soil stratigraphy below the foundation is qualitatively classified as a layered profile of sandy soils with silty or clay fines until 10 m depth, overlying a fine-grained soil deposit mainly silty between 10 and 16 m and mainly clayey deeper than 16 m (Figure 5a). Quantitative indications of the soil properties are obtained through four Standard Penetration Tests (SPT) carried out up to 5 to 20 m depth from the ground level, performed beneath four corners of the building (Figure 5b). Only two of them exceeded 6 m from the surface and are considered in the following. An average value of 10 is observed in the first 10 m, while the number of blow counts increases with the depth beyond 10 m (Figure 5b).

LIQUEFACTION ASSESSMENT

To back-analyze the observed phenomena, a two-step procedure was adopted. The first step consisted of the estimation of the liquefaction potential of the underlying soil layers by calculation of the safety factor against liquefaction based on the SPT-empirical chart proposed by Boulanger & Idriss (2014). The second step consisted of preliminary estimation of the earthquake-induced excess pore water pressure by using a simplified relationship based on the safety factor.

Safety factor against liquefaction

For defining the seismic demand, the maximum peak ground acceleration recorded at station 3513 has been adopted, which is equal to 0.12 g along the 27.4° N-W direction, and the moment magnitude of 6.6. The calculation of the Cyclic Stress Ratio (CSR) was performed according to the relationship:

$$\mathrm{CSR} = 0.65\frac{\tau_{max}}{\sigma'_v} = 0.65 \cdot \frac{a_{max}}{g} \cdot \frac{\sigma_v}{\sigma'_v} \cdot r_d \quad (1)$$

where the coefficient 0.65 is introduced to transform the irregular shear stress history (represented by τ_{max}) in one having an equivalent constant shear stress amplitude, σ_v and σ'_v are the vertical total and effective stresses at a depth z, a_{max} is the maximum horizontal acceleration, g is the gravity acceleration and r_d is a reduction factor accounting for soil deformability (Boulanger & Idriss, 2014).

For the estimation of the effective stress state of the foundation soil under static conditions, the load induced by the building was considered. Considering the stress transferred from the foundation per storey as 10 kPa (including the weight of mat foundation), total stress of 90 kPa can be calculated. Since the thickness of the sandy liquefiable layer is 7 m (Figure 5a), which is limited compared to the width of the foundation, an oedometric condition is assumed and the presence of the building was taken into account by adding the total stress to the geostatic stress state.

The Cyclic Resistance Ratio (CRR) of the foundation soils was calculated as a function of the corrected and normalized SPT blow count, $(N_1)_{60cs}$, according to the following equation:

$$CRR_{M=7.5,\sigma'=1} = \exp\left(\frac{(N_1)_{60cs}}{14.1} + \left(\frac{(N_1)_{60cs}}{126}\right)^2 - \left(\frac{(N_1)_{60cs}}{23.6}\right)^3 + \left(\frac{(N_1)_{60cs}}{25.4}\right)^4 - 2.8\right) \quad (2)$$

where $(N_1)_{60cs}$ is normalized and corrected SPT blow count.

The definition of $(N_1)_{60cs}$ requires the estimation of the fines content of each soil layer. In absence of a measured fines content, an estimation equal to 25% was assumed in the computation for the sandy soil based on the geological information. The profiles of corrected blow counts and the safety factor (SF) calculation are reported in Figures 5c and 5d, respectively. The liquefaction was not attained even though the FS is slighter than one at the depth of 7 m (Figure 5d). In the soil layer where the vertical drains are installed, the safety factor has an average value of 1.5.

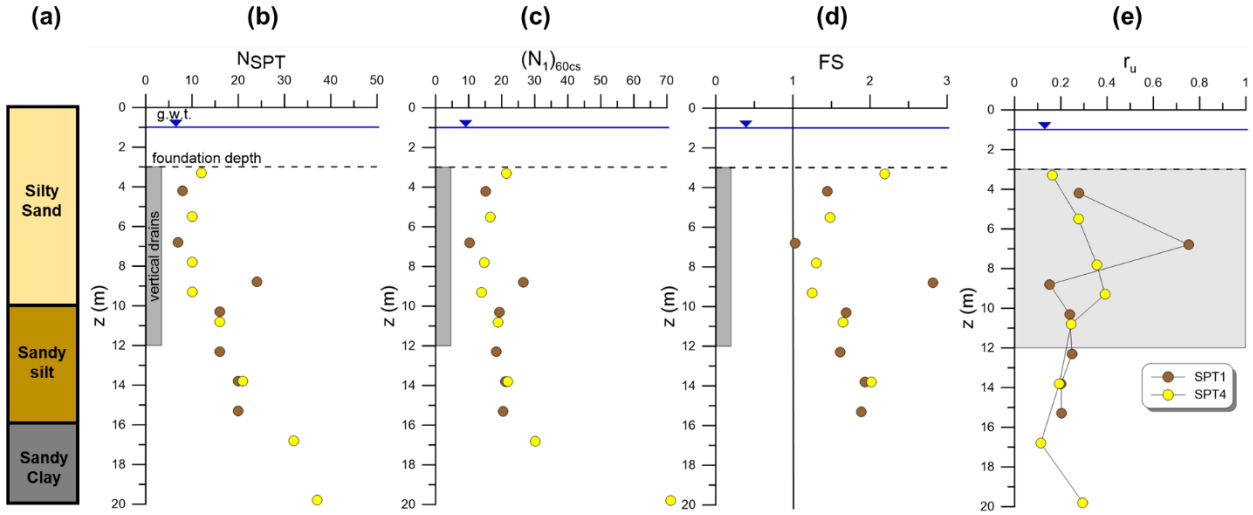

Figure 5. *Soil stratigraphy (a) with vertical profiles of measured SPT blow count (b), corrected SPT blow count (c), safety factor against liquefaction (d), and pore water pressure ratio estimation (e)*

Excess pore water pressure estimation

The obtained safety factor against liquefaction was used to perform a rough estimation of the seismic induced excess pore pressure ratio (r_u), defined as the ratio between the generated excess pore water pressure and the initial effective vertical stress. The analytical expression is as follow (Chiaradonna & Flora, 2019; Chiaradonna et al., 2019):

$$r_u = \frac{2}{\pi}\arcsin\left[FS^{-\frac{1}{2b\beta}}\right] \quad \text{for } FS > 1 \quad (3)$$

where the exponents b and β were defined as a function of normalized SPT blow count, $(N_1)_{60cs}$, and estimated fines content, FC (Chiaradonna & Flora, 2019). Figure 5e shows the vertical profile of the estimated pore pressure ratio. The estimated r_u is between 0.1 and 0.4, except for the layer at 7 m depth where a peak value of 0.8 is attained. This result is enough to induce a hydraulic gradient of 3 – 6 m of the water column and to justify the trigger of the vertical drains.

CONCLUSIONS

This paper documented the pore water pressure build-up observed in the Bayrakli district after the October 30, 2020 Samos earthquake. Approximate properties of the foundation soils were defined based on a fragmentary reconstruction of the field investigation performed before the construction of the building. Assessment of the safety factor against liquefaction is consistent with the absence of liquefaction manifestation in the area. Simplified prediction of the expected excess pore water pressure by use of a simple relationship based on the safety factor justified the mechanism that is behind the observed phenomenon. This methodology is particularly convenient because it can be directly applied to the safety factor.

The collection of additional geological and geotechnical data is currently in progress, and it will provide a better characterization of the foundation soils in Bayrakli while allowing the adoption of more sophisticated calculation methods (Chiaradonna et al., 2020) for the analysis of the rise of water in stone columns, associated with earthquake-induced pore water pressure development.

The back-analysis of the documented case history is of great importance in view of future near-field earthquakes (from the active faults surrounding the city of Izmir) that may portend an extremely worrying situation for a greater number of fatalities and much more significant damage, including liquefaction. Finally, it also represents a good benchmark to assess the efficacy of the simplified liquefaction vulnerability indexes to correctly address the soil liquefaction potential.

ACKNOWLEDGEMENT

The leading author was supported by the Italian Ministry of Research through the ‘Attraction and International Mobility’ project.

REFERENCES

Boulanger, R. W., & Idriss, I. M. (2014). CPT and SPT based liquefaction triggering procedures. *Center for Geotechnical Modeling*, *April*, 134. http://nees.ucdavis.edu/publications/Boulanger_Idriss_CPT_and_SPT_Liq_triggering_CGM-14-01_2014.pdf

Boulanger, R. W., Mejia, L. H., & Idriss, I. M. (1997). Liquefaction at moss landing during Loma Prieta earthquake. *Journal of Geotechnical and Geoenvironmental Engineering*, *123*(5), 453–467.

Cetin, K Onder, Mylonakis, G., Sextos, A., & Stewart, J. P. (2020). Seismological and Engineering Effects of the M 7.0 Samos Island (Aegean Sea) Earthquake. *Hellenic Association of Earthquake Engineering: Athens, Greece*. https://doi.10.18118/G6H088

Cetin, Kemal Onder, Papadimitriou, A. G., Altun, S., Pelekis, P., Unutmaz, B., Rovithis, E., Akgun, M., Klimis, N., Askan, A., Ziotopoulou, K., Sezer, A., Kincal, C., Ilgac, M., Can, G., Cakir, E., Soylemez, B., Al-Suhaily, A., Elsaid, A., Zarzour, M., … Mylonakis, G. (2021). The role of site effects on elevated seismic demands and corollary structural damage during the October 30, 2020, M7.0 Samos Island (Aegean Sea) Earthquake. *Bulletin of Earthquake Engineering*. https://doi.org/10.1007/s10518-021-01265-z

Chiaradonna, A., d’Onofrio, A., & Bilotta, E. (2019). Assessment of post-liquefaction consolidation settlement. *Bulletin of Earthquake Engineering*, *17*(11). https://doi.org/10.1007/s10518-019-00695-0

Chiaradonna, A., & Flora, A. (2019). On the estimate of seismically induced pore-water pressure increments before liquefaction. *Geotechnique Letters*, *10*(2), 1–7. https://doi.org/10.1680/jgele.19.00032

Chiaradonna, Anna, Flora, A., d’Onofrio, A., & Bilotta, E. (2020). A pore water pressure model calibration based on in-situ test results. *Soils and Foundations*, *60*(2), 327–341. https://doi.org/10.1016/j.sandf.2019.12.010

Chiaradonna, A Karakan, E., Lanzo, G., Monaco, P., Sezer, A., & Karray, M. (2022). Role of Local Site Effects on Damage Distribution in Izmir Metropolitan Area During the October 30, 2020 Samos Earthquake. *Earthquake Spectra (under review)*.

Cubrinovski, M., Rhodes, A., Ntritsos, N., & Van Ballegooy, S. (2018). System response of liquefiable deposits. *Soil Dynamics and Earthquake Engineering*, *May*. https://doi.org/10.1016/j.soildyn.2018.05.013

Kalogeras, I., Melis, N. S., & Kalligeris, N. (2020). The earthquake of October 30th, 2020 at Samos, Eastern Aegean Sea, Greece. *Report Published at EMSC*.

Karakan, E & Altun, S. (2016). Liquefaction Behavior and Post-Liquefaction Volumetric Strain Properties of Low Plasticity Silt Sand Mixtures. *Teknik Dergi*, *27*(4), 7593–7617.

Karakan, E Chiaradonna, A., Monaco, P., Lanzo, G., Sezer, A., & Karray, M. (2021). Identification of the Site Effects induced by the 2020 Samos Earthquake in Izmir. *Mediterranean Geosciences Union Annual Meeting (MedGU-21)*.

Kayen, R. E., Mitchell, J. K., Seed, R. B., & Nishio, S. (1998). Soil liquefaction in the east bay during the earthquake. *US Geol. Surv. Prof. Pap*.

Mavroulis, S., Triantafyllou, I., Karavias, A., Gogou, M., Katsetsiadou, K.-N., Lekkas, E., Papadopoulos, G. A., & Parcharidis, I. (2021). Primary and secondary environmental effects triggered by the 30 October 2020, Mw= 7.0, Samos (Eastern Aegean Sea, Greece) earthquake based on post-event field surveys and InSAR analysis. *Applied Sciences*, *11*(7), 3281.

Özyalin, Ş., & Tunçel, A. (2021). Investigation of liquefaction potential distribution in the east of izmir bay using masw method and scenario earthquakes. *6th International Congress On Innovative Scientific Approaches, Samsun, Turkey, 19-20 December, Pp.*, 483–490.

Sahadewa, A., Irsyam, M., Hanifa, R., Mikhail, R., Pamumpuni, A., Nazir, R., Pramono, S., Sabaruddin, A., Faizal, L., Ridwan, M., Himawan, A., Simatupang, P., Alatas, I. M., Harninto, D. S., Djarwadi, D., Kartawiria, A., Djunaidy, M., Suhendra, I., Kawanda, A., & Widodo, Y. (2019). Overview of the 2018 palu earthquake. *Earthquake Geotechnical Engineering for Protection and Development of Environment and Constructions- Proceedings of the 7th International Conference on Earthquake Geotechnical Engineering, 2019*, 857–869.

Sezer, A. (2020). Personal communication.

Sezer, A., Altun, S., & Göktepe, A. B. (2008). Microzonation of liquefaction susceptibility in Northern Izmir. *Proceedings of the International Conference of Development of Urban Areas and Geotechnical Engineering. Saint Petersburg*, 455–460.

Uzelli, T., Bilgiç, E., Öztürk, B., Baba, A., Sözbilir, H., & Tatar, O. (2021). Effects of seismic activity on groundwater level and geothermal systems in İzmir, Western Anatolia, Turkey: The case study from October 30, 2020 Samos earthquake. *Turkish Journal of Earth Sciences*.